Optics Letters

High dynamic range and wavelength-reused bidirectional radio-over-fiber link

Nianqiang Li and Jianping Yao*

Microwave Photonics Research Laboratory, School of Electrical Engineering and Computer Science, University of Ottawa, Ottawa, Ontario K1N 6N5, Canada
**Corresponding author: jpyao@eecs.uottawa.ca*

Received 20 December 2018; revised 5 February 2019; accepted 6 February 2019; posted 8 February 2019 (Doc. ID 355803); published 5 March 2019

We propose and experimentally demonstrate a bidirectional radio-over-fiber (RoF) link based on a Sagnac loop incorporating a polarization modulator (PolM) to generate simultaneously a polarization-modulated optical signal and an unmodulated optical signal for wavelength reuse and for increasing the dynamic range. Thanks to the traveling-wave nature of the PolM, a polarization-modulated optical signal and an unmodulated optical signal are generated at the output of the Sagnac loop, which are combined at a polarizer and detected at a photodetector. By controlling the powers of the two optical signals, the third-order intermodulation distortion terms can be fully suppressed to increase the dynamic range for downstream transmission. The unmodulated optical signal is reused for upstream transmission. A bidirectional RoF link to transmit 2.5 Gb/s 16QAM downstream and upstream signals, and a 7.1 Gb/s 128 subcarrier orthogonal frequency division multiplexing 16QAM downstream and upstream signals using a single wavelength over a 10.5 km single-mode fiber are experimentally demonstrated. The transmission performance versus the dynamic range is also studied.

https://doi.org/10.1364/OL.44.001331

The distribution of radio signals over an optical fiber or radio over fiber (RoF) has been a subject of intensive research for the last three decades [1,2]. The key advantages of an RoF link include wideband width, low loss, and immunity to electromagnetic interference, as compared with a conventional copper cable link. Numerous solutions to improve the transmission performance of RoF links have been proposed [3–7]. To offer broadband wireless access, the incorporation of RoF into a wavelength-division-multiplexed passive optical network (WDM-PON), or radio over WDM-PON (RoWDM-PON), has been considered a solution. To reduce the complexity and the cost of a RoWDM-PON, it is highly desirable that all signal generation and processing functions are implemented at the central station (CS), and the base stations (BSs) are made simple and less costly. Wavelength reuse at a BS is an effective solution to simplify a BS, since no light source is needed. In addition, wavelength reuse will make BSs colorless; thus, all BSs can be made identical, which will significantly reduce the overall system cost. Different techniques have been proposed to achieve wavelength reuse. For example, through injection locking of a Fabry–Pérot laser diode [8], the information encoded in the downlink optical carrier can be erased and, thus, the wavelength can be reused. The use of gain-saturation in a reflective semiconductor optical amplifier [9] can also erase the downstream signal that is intensity-encoded in the optical carrier. However, the approaches in Refs. [8,9] require the downstream signal to have a low extinction ratio or small modulation depth, which may degrade the system performance. A phase-modulated downstream signal can be directly reused as an optical carrier to encode an intensity-modulated upstream signal [10]. The major limitation of this scheme is that the upstream signal may be degraded due to the chromatic dispersion of the fiber link.

On the other hand, the performance of an RoF link is directly related to its dynamic range. The inherent nonlinearity of a modulator will cause in-band nonlinear distortions, especially the third-order intermodulation distortion (IMD3) [11], which will degrade the transmission performance. Great efforts have been devoted to eliminating the IMD3 terms to achieve an RoF with a high spurious free dynamic range (SFDR). It has been experimentally demonstrated that the dynamic range of a conventional Mach–Zehnder modulator (MZM)-based RoF link can be improved by using post-compensation [12], but the bandwidth is limited due to the limited speed of the electronic circuit used for post-processing. The SFDR of an RoF link can be increased all optically by canceling the IMD3 terms with a wider bandwidth by employing a single-drive dual-parallel MZM [13] or a dual-parallel polarization modulator (PolM) [14]. The bidirectional use of a single PolM in a Sagnac loop has proved to be an effective way to improve the dynamic range [15,16].

The approaches reported in [11–16] can be used to increase the dynamic range, but no wavelength reuse has been implemented to jointly achieve an RoF link with wavelength reuse and with a high dynamic range, which are highly needed in RoF links to achieve high-performance signal transmission while reducing the complexity and cost of BSs [17].

In this Letter, we propose and experimentally demonstrate a bidirectional RoF link implemented based on a Sagnac loop incorporating a PolM to generate a polarization-modulated optical signal and an unmodulated optical signal to simultaneously achieve wavelength reuse and dynamic range enhancement. It should be noted that a PolM is a traveling-wave device that supports effective modulation if a lightwave is co-propagating with a microwave signal and no modulation if they are traveling along the opposite directions due to velocity mismatch. If a PolM is incorporated in a Sagnac loop, a polarization-modulated optical signal and an unmodulated optical signal will be generated. The combination of the two signals at a polarizer at a BS will cancel the IMD3 terms; thus, the SFDR is increased. The unmodulated optical signal can be selected at a BS by a polarization beam splitter (PBS) and be employed for wavelength reuse. The proposed RoF link is experimentally demonstrated. By controlling the powers of the two optical signals along the two orthogonal polarization directions, the IMD3 terms are fully suppressed, and the dynamic range for downstream transmission is improved. The unmodulated optical signal is reused for upstream transmission. A bidirectional RoF link to transmit a 2.5 Gb/s 16QAM downstream and upstream microwave vector signals, and a 7.1 Gb/s 128 subcarrier orthogonal frequency division multiplexing (OFDM) 16QAM downstream and upstream microwave vector signals, using a single wavelength over a single-mode fiber (SMF) of 10.5 km is experimentally demonstrated. The error vector magnitude (EVM) performance versus the dynamic range is also studied.

Figure 1 shows schematic diagram of the proposed bidirectional RoF link. At the CS, a lightwave from a tunable laser source (TLS, Anritsu MG9638A) with an output power of 8 dBm and a wavelength of 1550.56 nm is sent to a Sagnac loop via a polarization controller (PC1) and an optical circulator (OC). The optical carrier is split into two orthogonally polarized lightwaves by PBS1. PBS1, two other PCs (PC2 and PC3), and a PolM constitute the Sagnac loop. The PolM (Versawave) is a special phase modulator that performs phase modulation along the two principal axes, but with opposite modulation indices. In the Sagnac loop, the counter-clockwise (CCW) lightwave is effectively modulated, whereas the clockwise (CW) lightwave is unmodulated due to the velocity mismatch. The CW and CCW signals that are orthogonally polarized are combined at PBS1 and sent to port 2 of the OC. The combined optical signal is amplified and transmitted over a length of SMF before reaching a specific BS. At the BS, the optical signal received is split into two signals by an optical coupler. In the upper path, the received signal is applied to a polarizer (Pol) via a fourth PC (PC4), which is amplified by an erbium-doped fiber amplifier (EDFA1) and detected by a photodetector (PD1). In the lower path, the joint operation of a PC (PC5) and a PBS (PBS2) ensures that only the unmodulated CW optical signal from the Sagnac loop is selected. For the upstream transmission, the chosen carrier is sent to an MZM (bandwidth 20 GHz) via a PC (PC6). Here PC6 is used to make sure that the polarization direction is parallel to the principal axis of the MZM to minimize the polarization dependent loss. The modulated upstream signal is transmitted over another SMF to the CS and converted into an electrical signal by a second PD (PD2) after amplification by a second EDFA (EDFA2). As shown in Fig. 1, the polarization direction of the optical carrier is aligned at an angle of α with respect to the principal axis of PBS1, which can be tuned by tuning PC1, and both PC2 and PC3 will introduce a 45° rotation to the polarization directions of both the CW and CCW lightwaves. For ease of implementation, the Pol is controlled at an angle of 45° relative to one principal axis of PBS1. Mathematically, the electrical fields of the CW and CCW signals at port 2 of the OC can be written as [15]

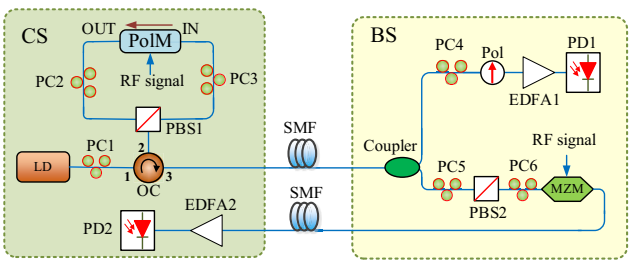

Fig. 1. Schematic diagram of the proposed bidirectional RoF link.

$$E_{\mathrm{CW}}(t) = E_0(t)\sin\alpha\cos\left(\frac{\varphi}{2}\right)\exp\left(\frac{j\varphi}{2}\right), \tag{1}$$

$$E_{\mathrm{CCW}}(t) = E_0(t)\cos\alpha\cos\left(\beta S(t)+\frac{j\varphi}{2}\right)\exp\left(\frac{j\varphi}{2}\right). \tag{2}$$

The two optical signals are combined at the Pol, and the resulting electrical field is given by [15]

$$\begin{aligned} E(t) &= E_{\mathrm{CCW}}\cos(45^\circ) + E_{\mathrm{CW}}\exp(j\theta)\sin(45^\circ) \\ &= \frac{1}{\sqrt{2}}E_0(t)\exp\left(\frac{j\varphi}{2}\right)\times\begin{bmatrix}\cos\alpha\cos\left(\beta S(t)+\frac{\varphi}{2}\right)\\ +\sin\alpha\cos\left(\frac{\varphi}{2}\right)\exp(j\theta)\end{bmatrix}, \end{aligned} \tag{3}$$

where $E_0(t)$ is the optical carrier from the TLS, $S(t)$ is the RF signal, β is the phase modulation index, and φ and θ are the polarization directions between the horizontal and vertical axes of the PolM and the principal axis of the polarizer, respectively.

To evaluate the IMD3 suppression, a two-tone analysis is performed. Assume an RF signal has two tones given by $S(t) = \cos(\omega_1 t) + \cos(\omega_2 t)$. After square-law detection at a PD and substituting the two-tone signal $S(t)$ into the resultant polynomial, a photocurrent is generated, given by

$$\begin{aligned} i_{AC}(t) &\propto E(t)E^*(t) \\ &\propto (\Gamma_1 + 3\Gamma_3)[\cos(\omega_1 t) + \cos(\omega_2 t)] \\ &\quad + \Gamma_3[\cos(2\omega_1 t - \omega_2 t) + \cos(2\omega_2 t - \omega_1 t)] + \ldots, \end{aligned} \tag{4}$$

where the coefficients Γ_1 and Γ_3 are given by

$$\Gamma_1 = -\sin\varphi\left[\frac{\beta}{2}\sin(2\alpha)\cos(\theta) + \beta\cos^2(\alpha)\right], \tag{5}$$

$$\Gamma_3 = \sin\varphi\left[\frac{\beta^3}{16}\sin(2\alpha)\cos(\theta) + \frac{\beta^3}{2}\cos^2(\alpha)\right]. \tag{6}$$

The comparison between Eqs. (5) and (6) indicates that one can simultaneously control α and θ via tuning the corresponding PCs to eliminate the IMD3 terms, but the fundamental terms are kept.

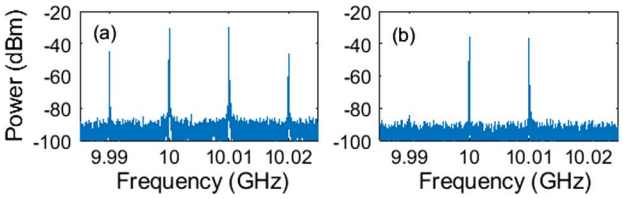

Fig. 2. Measured electrical spectra of the RF signal at the output of PD1 when a two-tone RF signal is applied to the PolM. (a) Weakly and (b) highly suppressed IMD3 terms.

Figure 2 shows two typical examples of the measured electrical spectra with strong and weak IMD3 terms by adjusting the PCs. In our experiment, a two-tone microwave signal at two frequencies of 10 and 10.01 GHz generated by an arbitrary wave generator (AWG, Keysight M8195A) and combined by a power combiner is used to modulate the lightwave from the TLS at the PolM. The results show that the proposed approach indeed allows effective suppression of the IMD3 terms. In fact, in our experiment, an improvement in an SFDR of around 15 dB is achieved.

By utilizing the highly linearized link shown in Fig. 1, a proof-of-concept experiment for downstream and upstream transmission is performed. Two 10 GHz RF signals carrying a 625 Mbaud (2.5 Gb/s) 16QAM data are generated by the AWG and applied to the PolM and the MZM. Figures 3(a) and 3(b) display the optical spectra for the optical carrier generated by the TLS with a wavelength centered at 1550.56 nm and the modulated downstream signal. As can be seen from Fig. 3(b), the joint operation of the PolM, PC3, and PBS1 is equivalent to an intensity modulator biased at the quadrature point, and a double sideband plus carrier (DSB+C) signal is generated [15,16]. Figure 3(c) shows the optical spectrum measured at the output of PBS2. No sidebands are generated due to velocity mismatch, indicating that the system offers a clear optical carrier for colorless upstream transmission. Figure 3(d) shows the optical spectrum measured at the output of the MZM biased at the quadrature point. It is clearly seen that the upstream microwave vector signal has been effectively modulated on the reused optical carrier.

Figure 4 shows the constellation diagrams of the received downstream and upstream signals with or without downstream interference for back-to-back (BTB) and 10.5 km SMF transmission. The bit rate for the downstream and upstream signals is 2.5 Gb/s, and the optical powers at the inputs of the PDs are 0 dBm. The clear constellations and the low values of the EVMs indicate good performance of the recovered signals in all cases considered. Thanks to the pure optical carrier for

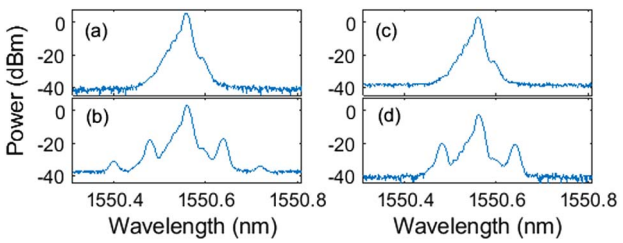

Fig. 3. Optical spectra measured (a) at the output of the TLS (b) before PD1, (c) before the MZM, and (d) after the MZM.

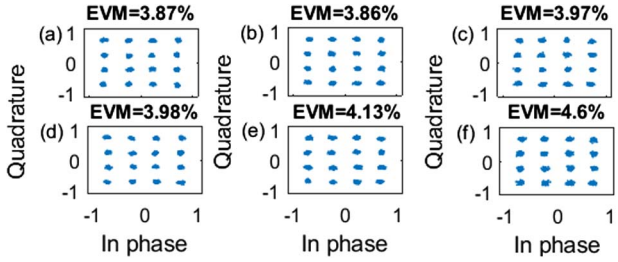

Fig. 4. Constellations for (up) BTB and (bottom) 10.5 km transmission: (a), (d) the downstream signal; (b), (e) the upstream signal without a downstream signal; and (c), (f) the upstream signal with a downstream signal. The optical power at the input of both PDs is 0 dBm.

upstream transmission, the signal degradation due to crosstalk between the downstream and upstream link is very small.

To further evaluate the transmission performance, the EVM versus the received optical power is measured. As shown in Fig. 5(a), the measured EVM of the downstream transmission is decreased from ~15% to below 4%, as the received optical power is increased from −9 to 0 dBm. This is expected, since a higher optical power improves the signal-to-noise ratio (SNR), which is essential for a better transmission performance with a smaller EVM. Figure 5(a) also confirms that the signal degradation due to fiber transmission is very small and can be ignored for the considered range of the received optical power in the downstream link. Figure 5(b) shows the results for the upstream link. As can be seen, the crosstalk from the downstream signal is small and negligible, which benefits from the high purity of the optical carrier for wavelength reuse. In contrast, the upstream transmission is more sensitive to the fiber link loss. However, the fiber-induced degradation is still acceptable in the whole range of the received optical power considered. In particular, the performance is comparable to that for the downstream transmission when the received optical power is sufficiently large, where an error-free transmission for both directions is ensured.

To demonstrate that the proposed RoF link supports other modulation formats, an additional experiment to transmit 16QAM-OFDM signals is performed. In the experiment, two OFDM signals with 256 IFFT length and 128 subcarriers at 4 GHz for downlink and uplink transmission, are generated by the AWG. Note that 16QAM-OFDM modulation is selected for all subcarriers with 1/8 cyclic prefix, resulting in

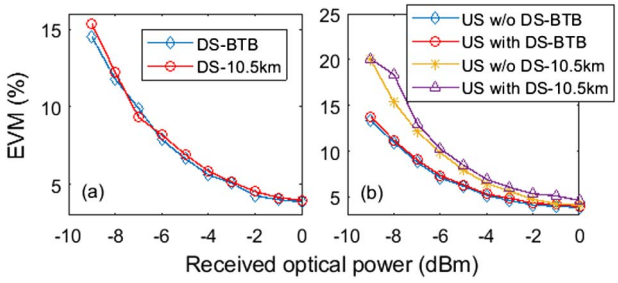

Fig. 5. EVMs versus the received optical power for BTB and 10.5 km transmission. (a) Downstream (DS) and (b) upstream (US) with or without DS.

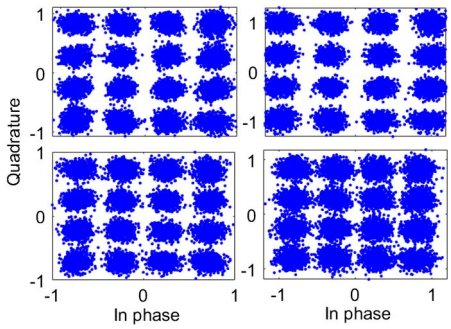

Fig. 6. Constellations of the 16QAM-OFDM signals for both downlink (left) and uplink (right) transmission. The optical powers at the inputs of the two PDs are 0 (upper) and −2 dBm (lower).

a total capacity of 7.1 Gb/s. After 10.5 km SMF transmission for both the downlink and uplink, the microwave vector signals are detected and recovered through offline digital signal processing. As shown in Fig. 6, clear constellations at two power levels are observed, which confirm the feasibility of the proposed scheme to serve as an OFDM-RoF link.

We then investigate the impact of the dynamic range improvement on the transmission performance of the RoF link. It was reported that an improved SFDR will lead to a better transmission performance [13,18]. Here we investigate the impact of the IMD3 on the transmission performance of the recovered microwave vector signal, which is evaluated in terms of the EVM. In the experiment, two microwave vector signals are again generated and transmitted. Specifically, we generate a 16QAM and a QPSK signals with their microwave carrier frequencies at 10 and 10.1 GHz, respectively. A bit rate of 50 Mbaud is set for both vector signals in order to minimize the spectral overlap. The optical power at the input of PD1 is set to be 0 dBm, and the PCs (PC1 and PC4) are controlled deliberately to obtain weakly, moderately, and highly suppressed IMD3 terms. Figure 7 shows three different levels of IMD3 cancellation and its inset show the corresponding constellation diagrams of the recovered 16QAM signal. The measured EVMs for the three cases are 3.69%, 6.44%, and 8.10%. In fact, the EVM is dependent on the electrical carrier-to-noise ratio (CNR) [19] given by

$$\mathrm{CNR} = \frac{(\beta R P_{\mathrm{sig}})^2/2}{\langle \Delta i^2_{\mathrm{shot}} \rangle + \langle \Delta i^2_{\mathrm{th}} \rangle + \langle \Delta i^2_{\mathrm{RIN}} \rangle + \langle \Delta i^2_{\mathrm{IMD3}} \rangle}, \quad (7)$$

where P_{sig} and $\langle \Delta i^2_{\mathrm{IMD3}} \rangle$ represent the average optical power and the intermodulation noise, respectively; $\langle \Delta i^2_{\mathrm{shot}} \rangle$, $\langle \Delta i^2_{\mathrm{th}} \rangle$, and $\langle \Delta i^2_{\mathrm{RIN}} \rangle$ are the shot, thermal, and relative intensity noises, respectively; and β and R are the modulation index and the PD1 responsivity. In our system, the terms in Eqs. (5) and (6) mainly contribute to P_{sig} and $\langle \Delta i^2_{\mathrm{IMD3}} \rangle$, respectively. As can be seen in Eq. (7), the CNR (in an analogy to a SNR) decreases with the increase in the IMD3, so that worse demodulation performance is expected for the case in which the IMD3 is large. This confirms the tendency observed in Fig. 7 and the significance of the proposed RoF link allowing

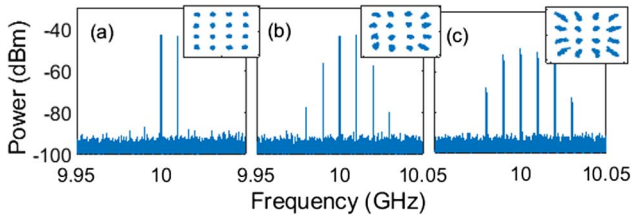

Fig. 7. Measured spectra of the RF signal. Inset: the constellations.

for wavelength reuse in conjunction with a high dynamic range with increased transmission performance.

In conclusion, we have experimentally demonstrated a bidirectional RoF link to offer simultaneously a high dynamic range and wavelength reuse. The IMD3 terms could be completely suppressed and, thus, the SFDR could be greatly improved when compared to a conventional RoF link. By utilizing a highly linearized RoF link, experiments to demonstrate wavelength reuse by transmitting 16QAM and 16QAM-OFDM signals for both downlink and uplink were performed. The proposed system requires no additional laser source or filter at the BS and, thus, is simple, colorless, and compatible with prevailing WDM-PONs.

Funding. Natural Sciences and Engineering Research Council of Canada (NSERC).

REFERENCES

1. J. Capmany and D. Novak, Nat. Photonics **1**, 319 (2007).
2. J. Yao, J. Lightwave Technol. **27**, 314 (2009).
3. X. Chen and J. Yao, IEEE Photonics Technol. Lett. **29**, 1071 (2017).
4. B. Wu, M. Zhu, J. Zhang, J. Wang, M. Xu, F. Yan, S. Jian, and G.-K. Chang, Opt. Express **23**, 18323 (2015).
5. S. Liu, P.-C. Peng, M. Xu, D. Guidotti, H. Tian, and G.-K. Chang, IEEE Photonics Technol. Lett. **30**, 1396 (2018).
6. K. Van Gasse, J. Van Kerrebrouck, A. Abbasi, J. Verbist, G. Torfs, B. Moeneclaey, G. Morthier, X. Yin, J. Bauwelinck, and G. Roelkens, J. Lightwave Technol. **36**, 4438 (2018).
7. F. Xiong, W.-D. Zhong, and H. Kim, J. Lightwave Technol. **30**, 355 (2012).
8. W. Cui, T. Shao, and J. Yao, J. Lightwave Technol. **32**, 220 (2014).
9. T. Y. Kim and S. K. Han, IEEE Photonics Technol. Lett. **18**, 2350 (2006).
10. J. Zheng, H. Wang, L. Wang, N. Zhu, J. Liu, and S. Wang, Opt. Lett. **38**, 1167 (2013).
11. Y. Gao, A. Wen, L. Liu, S. Tian, S. Xiang, and Y. Wang, J. Lightwave Technol. **33**, 2899 (2015).
12. G. Zhang, S. Li, X. Zheng, H. Zhang, B. Zhou, and P. Xiang, Opt. Express **20**, 17214 (2012).
13. S. Li, X. Zheng, H. Zhang, and B. Zhou, IEEE Photonics Technol. Lett. **22**, 1775 (2010).
14. M. Huang, J. Fu, and S. Pan, Opt. Lett. **37**, 1823 (2012).
15. W. Li, X. Wang, and N. Zhu, IEEE Photonics Technol. Lett. **26**, 89 (2014).
16. W. Li and J. Yao, Opt. Express **21**, 15692 (2013).
17. H.-H. Lu, S.-J. Tzeng, and Y.-L. Liu, IEEE Photonics Technol. Lett. **16**, 602 (2004).
18. Z. Chen, L. Yan, W. Pan, B. Luo, X. Zou, Y. Guo, H. Jiang, and T. Zhou, Opt. Express **21**, 20999 (2013).
19. J. M. Galve, I. Gasulla, S. Sales, and J. Capmany, J. Lightwave Technol. **52**, 0600507 (2016).